



Gravitational Wave Parameter Estimation

Jack Tobin

A thesis presented for the degree of Applied and Computational
Mathematics
Bachelor of Science Honours (BSc Hons.)

School of Mathematics and Statistics
University College Dublin (U.C.D.)

Acknowledgements

I am immensely grateful to my supervisor, Dr. Sarp Akcay, for being incredibly generous with both his time and knowledge. His advice and mentorship was invaluable and made the project thoroughly enjoyable. I'd also like to thank my parents, Kathleen Ryan and P.J. Tobin, for their unwavering support throughout my studies.

Contents

| | | |
|----------|---|-----------|
| 1 | Introduction | 6 |
| 2 | Gravitational Waves | 7 |
| 2.1 | Linearized Theory | 7 |
| 2.2 | Gravitational Wave Frequency of Binary Black Hole Inspirals | 9 |
| 2.2.1 | Newtonian Evolution | 9 |
| 3 | Detection of Gravitational Waves | 12 |
| 3.1 | LIGO and Virgo Detectors | 12 |
| 3.2 | Matched Filtering | 13 |
| 4 | Bayesian Probability Theory | 16 |
| 4.1 | Bayes' Theorem | 16 |
| 4.2 | Markov Chain Monte Carlo Methods | 17 |
| 4.2.1 | PyCBC | 17 |
| 5 | Binary Black-Hole Merger Events | 18 |
| 5.1 | GW150914 | 18 |
| 5.1.1 | Results | 19 |
| 5.2 | GW170814 | 23 |
| 5.2.1 | Results | 25 |
| 5.3 | GW190521B | 29 |
| 5.3.1 | Results | 31 |
| 6 | Conclusions and Further Scope | 36 |

List of Figures

| | | |
|------|--|----|
| 3.1 | A basic schematic of a Michelson Interferometer: Source [2] | 13 |
| 3.2 | LIGO Detector Strain Data. Source [3] | 14 |
| 5.1 | Source-frame mass posteriors for GW150914 obtained using the IMRPhenomXPHM model. \mathcal{M} here represents the chirp mass. | 19 |
| 5.2 | GW150914 primary source masses estimated with the NRSur7dq4 model. | 20 |
| 5.3 | GW150914 posterior distributions for the masses estimated with the IMRPhenomPv2 model. | 21 |
| 5.4 | Spins and redshift posterior distributions for GW150914 using the IMRPhenomPv2 Model. | 22 |
| 5.5 | Posterior primary source mass distribution for GW150914 constructed from the posterior distributions of all three models. The sharp diagonal line in the upper left corner of the scatter plot is a consequence of the requirement that $m_1 \geq m_2$. | 23 |
| 5.6 | Mass Posterior Distributions for GW170814 estimated with the IMRPhenomXPHM model. | 25 |
| 5.7 | Masses for GW170814 estimated with NRSur7dq4 model. | 26 |
| 5.8 | GW170814 Masses Estimated with the IMRPhenomPv2 Model | 27 |
| 5.9 | Posteriors plotted for the spins and redshift for GW170814 using the IMRPhenomXPHM Model. | 28 |
| 5.10 | GW170814 Combined Posteriors for Masses. | 29 |
| 5.11 | GW190521B Masses estimated with the IMRPhenomXPHM Model | 31 |
| 5.12 | GW190521B Masses estimated with the NRSur7dq4 Model | 32 |
| 5.13 | GW190521B Masses estimated with the IMRPhenomPv2 Model. | 33 |
| 5.14 | GW190521B's spins and redshift estimated with the NRSur7dq4 Model. | 34 |

| | |
|--|----|
| 5.15 GW190521B posterior distribution for the combined source mass distributions of all three models. | 35 |
| 6.1 Histogram of the median value of the primary source masses for the 93 gravitational- wave events to date. | 36 |
| 6.2 Estimated Probability Density Function for the Primary Source Mass. | 38 |

List of Tables

| | | |
|-----|---|----|
| 5.1 | Median Values with 90% Confidence Intervals for Published GW150914 Parameters | 18 |
| 5.2 | Median Values with 90% Confidence Intervals for Published GW170814 Parameters | 24 |
| 5.3 | 90% Confidence Intervals for Published GW190521B Parameters | 30 |

Abstract

This project aims to explore the methods used in estimating the parameters of the sources that emit gravitational waves. I begin by briefly describing gravitational waves and the equations that govern them. This is followed by how gravitational waves are detected and the necessary theory used in estimating their parameters. Finally I present my analysis for the events GW150914, GW170814 and GW190521_074359.

Introduction

In 1915, Einstein first published his General Theory of Relativity. That theory led to a prediction of the existence of gravitational waves. He predicted that these waves, caused by some of the most fierce and energetic events in our universe, would cause 'ripples' in the fabric of space time. These cosmic ripples would propagate at the speed of light and carry with them information about their source[1]. However, as their effect on Earth would be so faint, Einstein himself wondered if it would ever be possible to detect their existence. However, exactly 100 years since Einstein published his theory, the first gravitational wave was detected on the 14th of September 2015 [9]. Since then, the detection of gravitational waves has become commonplace with over 90 detections to date. These detections alone do not inform us about the sources emitting them. Estimating the parameters of the sources involves subtracting a theoretical waveform model from the detector data, provided by the gravitational wave detectors such as LIGO and Virgo, and examining if the remainder is white noise. Before conducting any parameter estimation it is crucial to understand the equations that dictate gravitational waves and this will be the subject of discussion in the following section.

Gravitational Waves

This section introduces ‘linearized theory’ of general relativity to describe gravitational waves. This results from expanding the Einstein equations around the flat Minkowski space metric. This approach allows us to see how gravitational waves form. It also enables us to express solutions to the wave equation in a concise and simple form by making an appropriate gauge choice. The following section is adapted from Michele Maggiore’s book “Gravitational Waves” [15].

2.1 Linearized Theory

We begin with the Einstein field equations

$$R_{\mu\nu} - \frac{1}{2}g_{\mu\nu}R = \frac{8\pi G}{c^4}T_{\mu\nu}, \quad (2.1)$$

where R is the Ricci scalar and $R_{\mu\nu}$ is the Ricci tensor, and $T_{\mu\nu}$ is the energy-momentum tensor of matter. General relativity is invariant under the group of all possible coordinate transformations,

$$x^\mu \rightarrow x'^\mu(x). \quad (2.2)$$

If $x'^\mu(x)$ is taken to be an arbitrary diffeomorphism , i.e. that $x'^\mu(x)$ is invertible, differentiable and has a differentiable inverse, then under this transformation the metric transforms as follows,

$$g_{\mu\nu}(x) \rightarrow g'_{\mu\nu}(x) = \frac{\partial x^\rho}{\partial x'^\mu} \frac{\partial x^\sigma}{\partial x'^\nu} g_{\rho\sigma}(x). \quad (2.3)$$

To analyse the gravitational waves, we are interested in regions away from the source of the mass/energy so we expect to be in weak field gravity. The metric is then described by small

perturbations from the flat Minkowski space-time:

$$g_{\mu\nu} = \eta_{\mu\nu} + h_{\mu\nu} \quad (2.4)$$

Where $\eta_{\mu\nu}$ is the Minkowski metric and $h_{\mu\nu}$ are small perturbations such that $h_{\mu\nu} \ll 1$.

Now consider the coordinate transformation given by

$$x^\mu \rightarrow x'^\mu = x^\mu + \zeta^\mu(x). \quad (2.5)$$

Using the transformation law of the metric from equation (2.3), we find that the transformation of $h_{\mu\nu}$, to the lowest order is

$$h_{\mu\nu}(x) \rightarrow h'_{\mu\nu}(x') = h_{\mu\nu}(x) - (\partial_\mu \zeta_\nu + \partial_\nu \zeta_\mu). \quad (2.6)$$

This equation enables us the freedom to choose our gauge. To linear order in $h_{\mu\nu}$, the Riemann tensor becomes

$$R_{\mu\nu\rho\sigma} = \frac{1}{2}(\partial_\nu \partial_\rho h_{\mu\sigma} + \partial_\mu \partial_\sigma h_{\nu\rho} - \partial_\mu \partial_\rho h_{\nu\sigma} - \partial_\nu \partial_\sigma h_{\mu\rho}). \quad (2.7)$$

Using the above equation we can now find the linearization of the Einstein tensor to obtain the linearization of the Einstein equations,

$$\square \bar{h}_{\mu\nu} + \eta_{\mu\nu} \partial^\rho \partial^\sigma \bar{h}_{\rho\sigma} - \partial^\rho \partial_\nu \bar{h}_{\mu\rho} - \partial^\rho \partial_\mu \bar{h}_{\nu\rho} = -\frac{16\pi G}{c^4} T_{\mu\nu}. \quad (2.8)$$

Here \square is taken to be the flat space d'Alembertian. $\bar{h}_{\mu\nu}$ represents a gravitational wave propagating at the speed of light within a flat Minkowski space-time. From equation (2.6) we have the freedom to choose our gauge. Making the choice of the Lorenz gauge, i.e., $\partial_m u \bar{h}^{\mu\nu} = 0$, leads us to the simplified expression

$$\square \bar{h}_{\mu\nu} = -\frac{16\pi G}{c^4} T_{\mu\nu}. \quad (2.9)$$

We are interested in the region far away from any sources of gravity, so $T_{\mu\nu} = 0$. This leads us to the further simplified wave equation

$$\square \bar{h}_{\mu\nu} = 0. \quad (2.10)$$

Given that $\square = -(\frac{1}{c^2})\partial_t^2 + \nabla^2$, solutions to Eq. 2.10 yield gravitational waves that propagate at the speed of light. Furthermore, by choosing the Lorentz gauge we reduce the degrees of freedom of the matrix $h_{\mu\nu}$ to two degrees of freedom. These degrees of freedom manifest themselves as the + and \times polarizations of the wave.

2.2 Gravitational Wave Frequency of Binary Black Hole Inspirals

This section details the frequency evolution of gravitational waves for compact binary inspirals where the systems are composed of black holes and/or neutron stars. The following derivations have been adapted from Ref. [7].

2.2.1 Newtonian Evolution

We begin with the famous Einstein Quadrupole formula. The power emitted in gravitational waves is given by

$$\dot{E} = \frac{G}{5c^5} \langle \ddot{Q}_{ij} \ddot{Q}_{ij} \rangle. \quad (2.11)$$

Q_{ij} is a trace-reversed mass quadrupole moment. We can simplify this expression by assuming the binary system to be two point-masses in a circular orbit around a common centre of mass. For a binary system with Keplerian orbital angular frequency Ω , relative separation r and masses $m_1 \geq m_2$, Eq. (2.11) becomes

$$\dot{E} = \frac{32}{5} \frac{G\mu^2}{5c^5} r^4 \Omega^6. \quad (2.12)$$

where $\mu = \frac{m_1 m_2}{M}$ is the reduced mass and M is the total mass. Then by using Kepler's third law, $\Omega^2 = GMr^{-3}$, Eq. 2.12 can then be expressed as function of constants and ω ,

$$\dot{E} = \frac{32}{5} \frac{c^5}{G} \left(\frac{GM_c \omega}{2c^3} \right)^{\frac{10}{3}}. \quad (2.13)$$

Where,

$$\mathcal{M}_c = \frac{(m_1 m_2)^{\frac{3}{5}}}{(m_1 + m_2)^{\frac{1}{5}}}. \quad (2.14)$$

\mathcal{M}_c is the so called 'Chirp Mass'. The combination of μ and M in Eq. 2.13 leads to \mathcal{M}_c having units of mass giving rise to the name. Here $\omega = 2\Omega$ is the angular frequency of the quadrupolar gravitational waves. The emission of power in gravitational waves decrease the total energy of the binary system, usually referred to as the binding energy given by

$$E_b = -\frac{Gm_1 m_2}{2r}. \quad (2.15)$$

Using Kepler's third law, $\Omega^2 = GMr^{-3}$, and the definition of the chirp mass, we can rewrite Eq. (2.15) as

$$E_b = -\left(\frac{G^2 M_c^5 \omega^2}{32} \right)^{\frac{1}{3}}. \quad (2.16)$$

Due to the conservation of energy, the power emitted in gravitational waves must be equal to the change of energy in the binary system, $\dot{E} = -\dot{E}_b$. Then by computing \dot{E}_b and setting this equal to Eq. (2.13), we obtain an expression for $\dot{\omega}$ as a function of ω and other fundamental constants. We can then take $\omega = 2\pi f$ to arrive at the expression for the evolution of the frequency of gravitational waves:

$$\dot{f} = \frac{96}{5} \pi^{\frac{8}{3}} \frac{(GM_c)^{\frac{5}{3}}}{c^5} f^{\frac{11}{3}} \quad (2.17)$$

This result will be of paramount importance in estimating the parameters of the sources of gravitational waves.

As a direct consequence of Eq. (2.17), the chirp mass \mathcal{M}_c will be the most accurately estimated parameter. Specifically because we can measure f very precisely and consequentially obtain \dot{f} very accurately also.

Detection of Gravitational Waves

Before moving forward to my analysis of the binary black hole merger events, I will briefly discuss how gravitational waves are detected. In this section I will describe the detector's architecture, its mechanics and the data obtained from them.

3.1 LIGO and Virgo Detectors

The data used in this project was obtained from the LIGO detectors, located in Hanford Washington and Livingston Louisiana USA, and the VIRGO detector located in Cascina Italy. Fundamentally, both the LIGO and VIRGO detectors are scaled up Michelson interferometers. The arms of LIGO and VIRGO are 4km and 3km, respectively. Interferometers get their name from the fact that they merge multiple sources of light together to create an interference pattern. These interference patterns created can then be used to gather information about the phenomena causing them.

Their structure is depicted in Fig. 3.1 below.

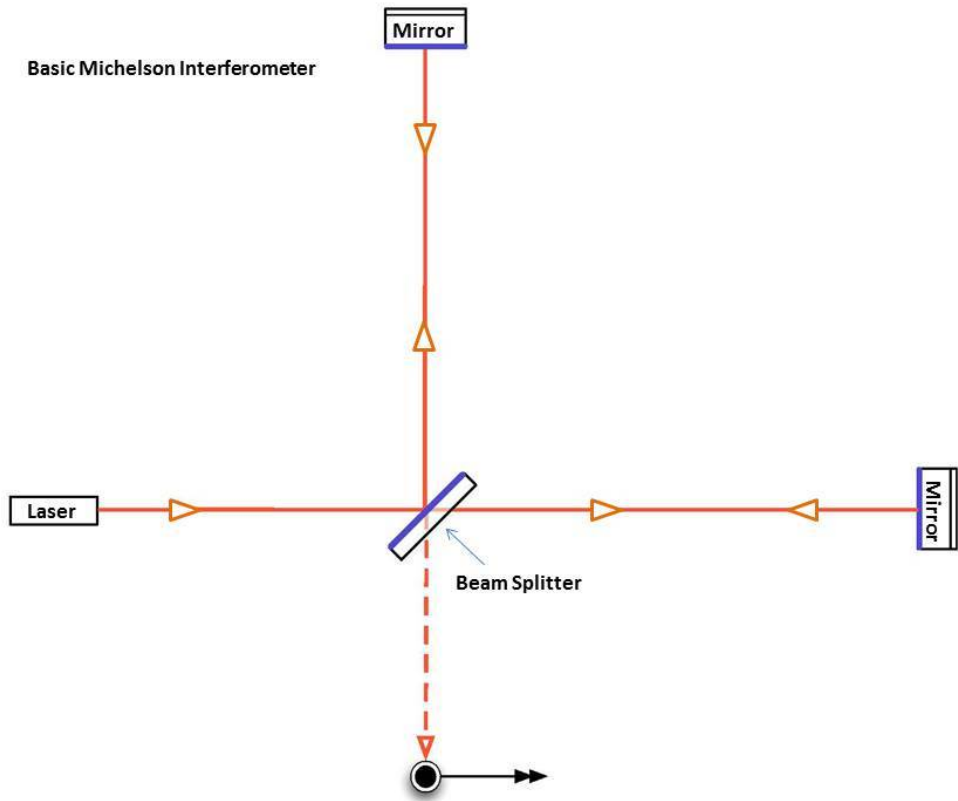


Figure 3.1: A basic schematic of a Michelson Interferometer: Source [2]

As a gravitational wave passes through the earth, it stretches and contracts the earth. In doing so, it also stretches and contracts the arms of the detector. This causes the waves of light from the lasers to have constructive and destructive interference with each other. This interference can then be measured to detect the passing of a gravitational wave. The change in arm length of the LIGO detectors can be as small as $1/10000^{th}$ the width of a proton [2].

3.2 Matched Filtering

The data we gather from the detectors is not a pure signal. The signal is noisy and we must process it in order to reduce errors in the parameter estimation. The data analysis technique ‘matched filtering’ is used to search for a signal of a known shape buried in noisy data [17]. This process is analogous to being able to recognize a song over a large crowd of people

talking. We obtain a signal $s(t)$ that contains a waveform $h(t)$ and some noise $n(t)$

$$s(t) = h(t) + n(t) \quad (3.1)$$

Fig. 3.2 shows a deconstructed signal for the event GW150914. At the top of the figure we have the raw signal which is also commonly referred to as the 'chirp signal', characterized by both its increase in frequency and amplitude. Underneath we have a theoretical waveform model. Lastly directly below we have the raw signal with the theoretical waveform subtracted from it leaving a residual white noise.

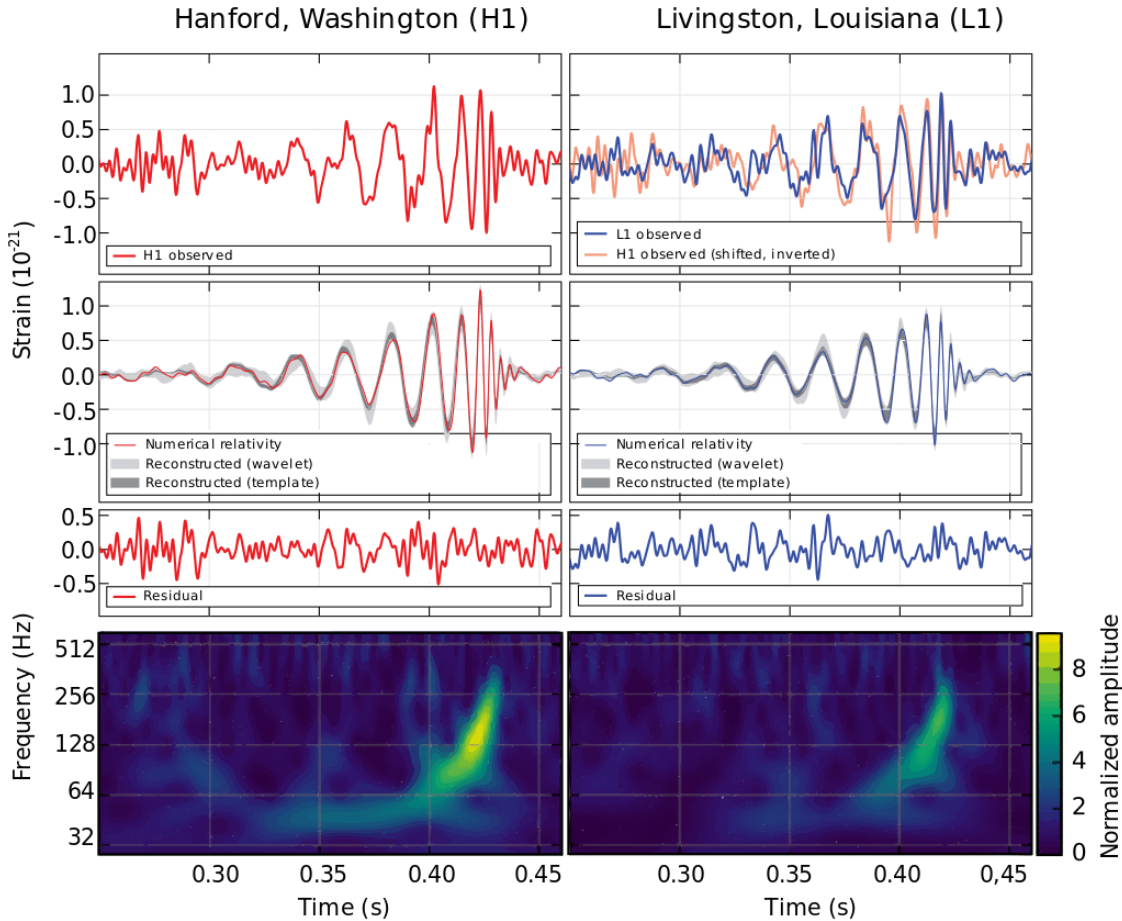


Figure 3.2: LIGO Detector Strain Data. Source [3].

The technique consists of correlating the output of a detector with a theoretical waveform, known as a template or a filter. Given a signal $h(t)$ buried in noise $n(t)$, the task is to

find an 'optimal' template $q(t)$ that would produce, on average, the best possible signal to noise ratio [17]. In practice however, the true waveform is not known and must be estimated using large-scale simulations [12]. The waveform is a function of at least 14 parameters If we then use 10 grid points per parameter in our estimation this would yield 10^{14} waveforms to be matched-filtered which is infeasible. The solution is to use Markov Chain Monte Carlo methods (MCMC) in order to efficiently walk through our parameter space [14]. I will further elaborate on MCMC methods in the following section.

Bayesian Probability Theory

We aim to estimate the parameters of the sources of gravitational wave given a signal from the detectors. Consequently, we must work within a Bayesian framework. A Bayesian framework enables us to take an observed result and work backwards via inference towards a possible cause [14].

4.1 Bayes' Theorem

Bayes' Theorem describes the probability of observing an event A given that an event B has occurred. This is given by the following equation,

$$P(A|B) = \frac{P(B|A)P(A)}{P(B)} \quad (4.1)$$

where $P(B)$ is the probability that event B has occurred and $P(B|A)$ is the probability that event B will occur given that event A already has. Within the context of gravitational wave parameter estimation, we hypothesise that the signal data we observe are the output of a theoretical waveform model \mathcal{M} which is parameterized by a vector of physical quantities $\vec{\theta}$ [14]. Eq (4.1) can be re-written as

$$p(\vec{\theta}|d, \mathcal{M}) = \frac{p(d|\vec{\theta}, \mathcal{M})p(\vec{\theta}, \mathcal{M})}{p(d, \mathcal{M})}. \quad (4.2)$$

Where d is the data. $p(\vec{\theta}|d, \mathcal{M})$ is known as the ‘posterior distribution’ and similarly $p(d, \mathcal{M})$ is known as the ‘prior’ distribution. This choice of prior distribution will ultimately affect the outcome of our posterior distribution. However, as we collect data from the posterior distribution this in turn can become the prior and lead to more informative results. I expand further upon this idea the in the conclusions section of this report.

4.2 Markov Chain Monte Carlo Methods

As mentioned previously, sampling directly from the parameter space of the posterior is infeasible for gravitational waveform models. MCMC enables us to travel through the parameter space in a more efficient manner. We start with a position $\vec{\theta}_i$ in the parameter space as the initial state in the Markov chain. A transition to a state θ_{i+1} is proposed using a normalized distribution $q(\vec{\theta}_i|\vec{\theta}_{i+1})$. This state is accepted with a probability $\kappa = [1, H]$, where H is the Hastings ratio:

$$H_{\vec{\theta}_i \rightarrow \vec{\theta}_{i+1}} = \frac{p(d|\vec{\theta}_{i+1})p(\vec{\theta}_{i+1})q(\vec{\theta}_i|\vec{\theta}_{i+1})}{p(d|\vec{\theta}_i)p(\vec{\theta}_i)q(\vec{\theta}_{i+1}|\vec{\theta}_i)}. \quad (4.3)$$

The above equation is effectively a modified version of Eq. (4.2). This ratio of the proposed state's probabilities will penalize areas of the parameter space that are frequently visited and will promote rarely suggested parts of the parameter space. The MCMC will accept proposed transitions to states with higher posterior weights and reject other states with lower weight [14]. Fortunately, there is a software library “PyCBC” that I used in my parameter estimation to handle all of the above computations.

4.2.1 PyCBC

PyCBC is a specific Python library for Compact Binary Calescences (CBCs). It is a free and open-source software package used to analyse gravitational wave data. The software includes algorithms to make Bayesian inferences, such as MCMC, from gravitational-wave data. PyCBC was used in the first direct detection of gravitational waves and is used in the continual analysis of the LIGO and VIRGO detector data [18].

Binary Black-Hole Merger Events

In this section, I will present my results for my analysis of the events GW150914, GW170814 and GW190521_074359 (GW190521B). All of the events were estimated using the PyCBC software package [16]. The prior distributions for all parameters and all events was taken to be uniformly distributed. Each event was estimated with three waveform models. IMRPhenomXPHM [13], NRSur7dq4 [19] and IMRPhenomPv2 [11].

5.1 GW150914

GW150914 was the first gravitational-wave ever to be detected. LIGO detected this gravitational-wave on the 14th of September 2015. It is a binary black-hole merger event with a signal to noise ratio of 24.4. Table 5.1 below details the published median values with 90% confidence intervals of the parameters for the event GW150914 [4]. This is directly followed by the estimates from my analysis of the event.

Table 5.1: Median Values with 90% Confidence Intervals for Published GW150914 Parameters

| | |
|---|---------------------------|
| Source-frame primary mass $m_1^{\text{source}}/M_{\odot}$ | $35.8^{+5.3}_{-3.9}$ |
| Source-frame secondary mass $m_2^{\text{source}}/M_{\odot}$ | $29.1^{+3.8}_{-4.3}$ |
| Source-frame chirp mass $\mathcal{M}_c^{\text{source}}/M_{\odot}$ | $28^{+2.0}_{-1.7}$ |
| Dimensionless primary spin magnitude a_1 | $0.32^{+0.49}_{-0.29}$ |
| Dimensionless secondary spin magnitude a_2 | $0.44^{+0.5}_{-0.4}$ |
| Source redshift z | $0.088^{+0.032}_{-0.037}$ |

5.1.1 Results

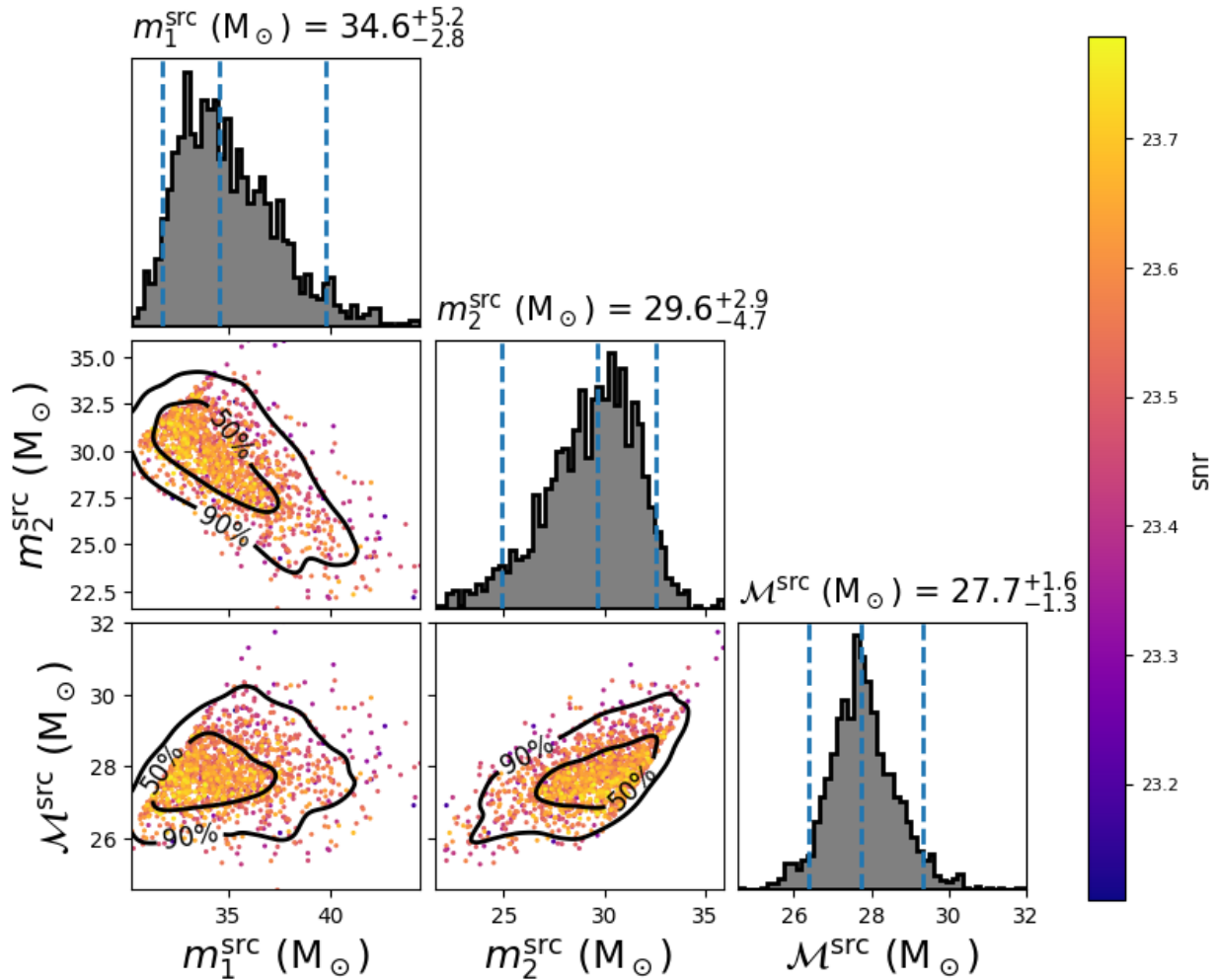


Figure 5.1: Source-frame mass posteriors for GW150914 obtained using the IMRPhenomX-PHM model. \mathcal{M} here represents the chirp mass.

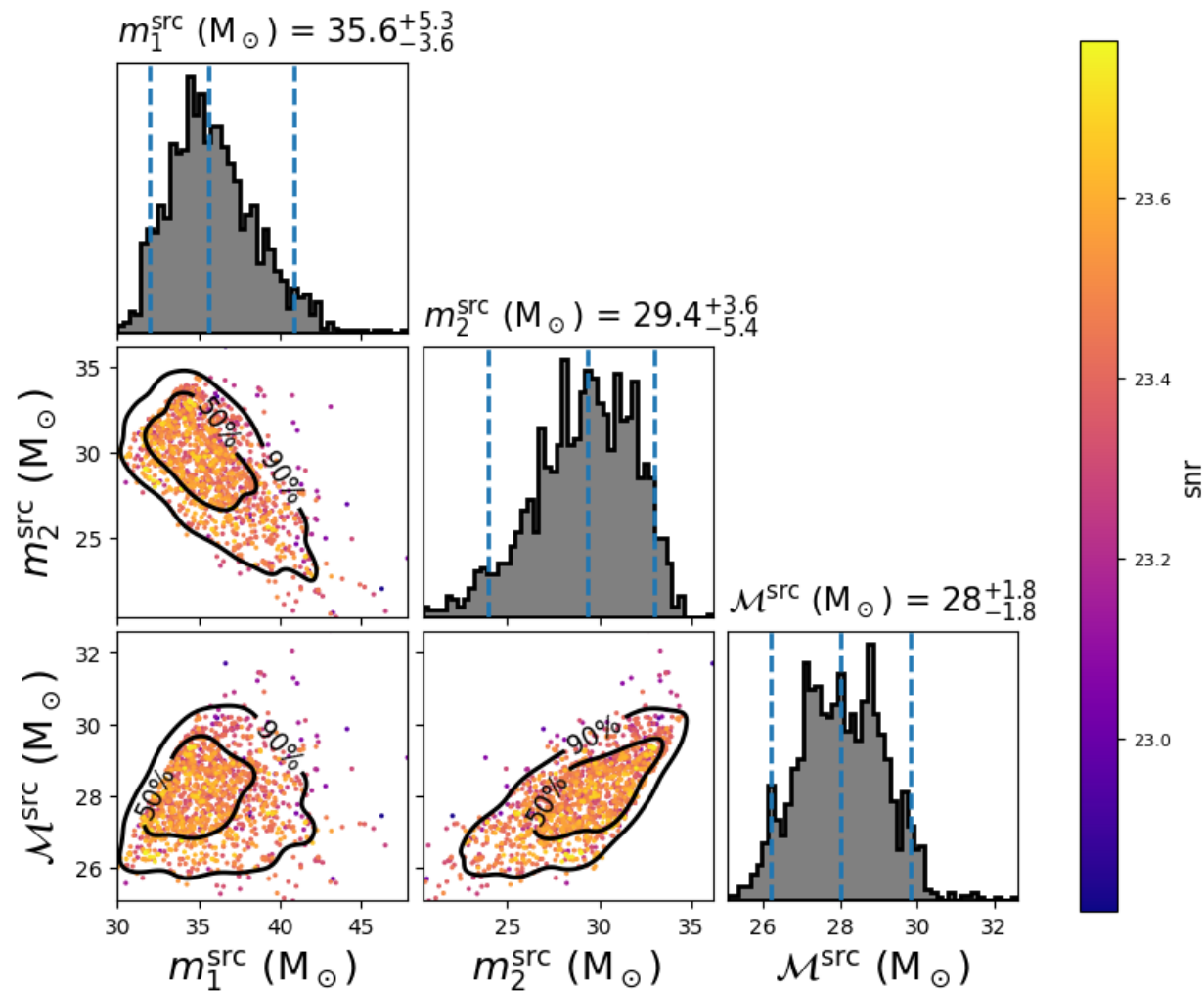


Figure 5.2: GW150914 primary source masses estimated with the NRSur7dq4 model.

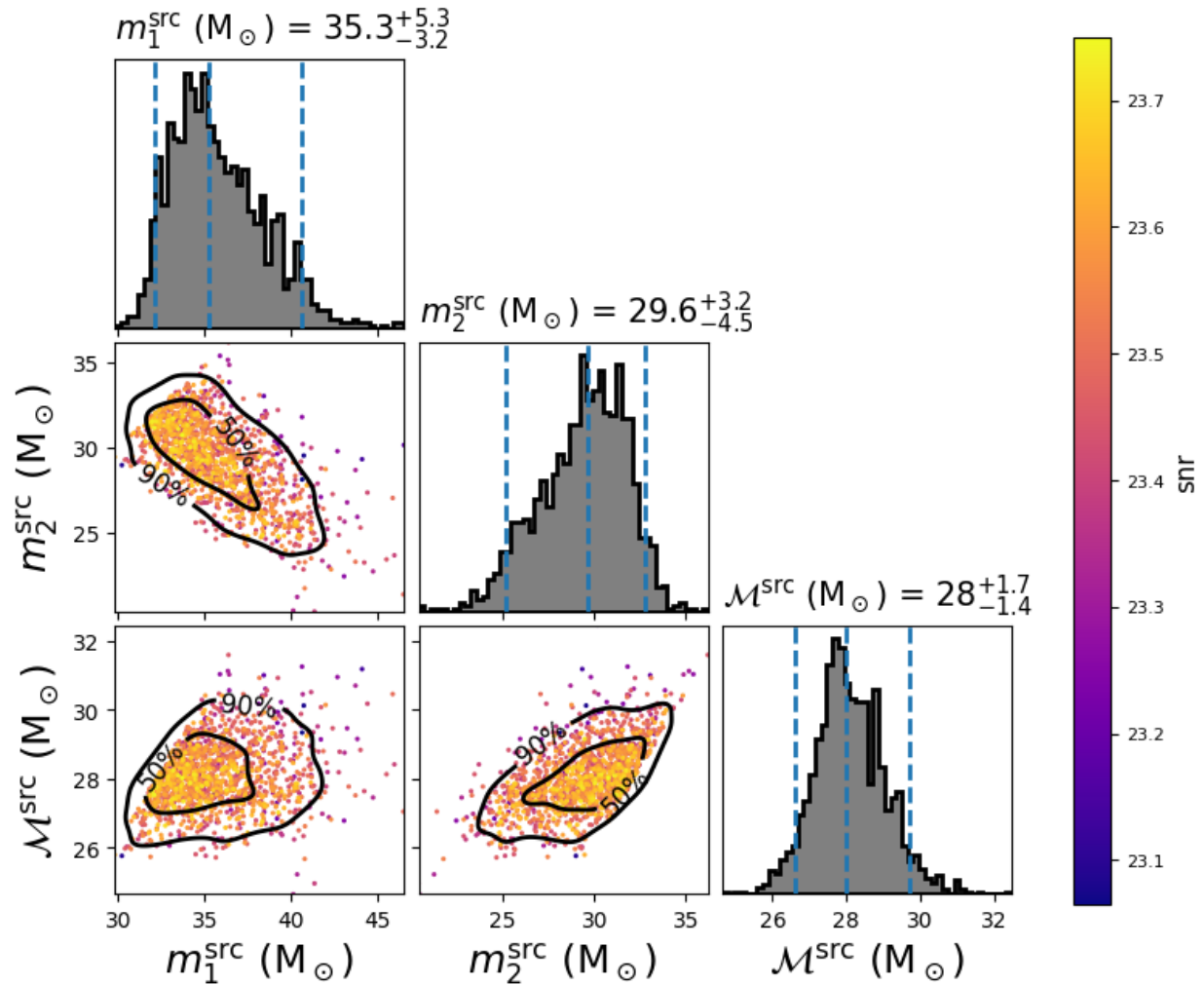


Figure 5.3: GW150914 posterior distributions for the masses estimated with the IMRPhenomPv2 model.

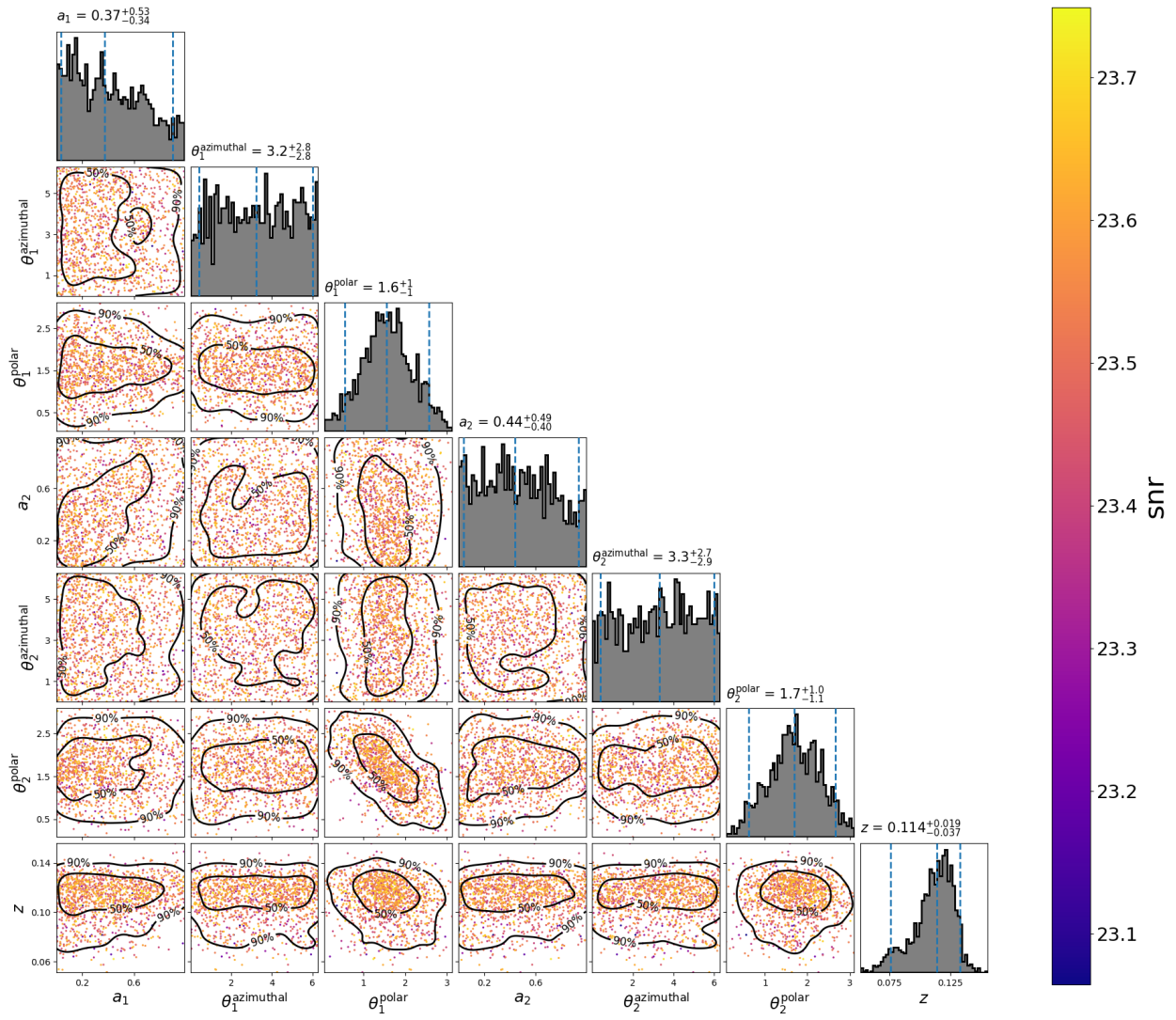


Figure 5.4: Spins and redshift posterior distributions for GW150914 using the IMRPhenomPv2 Model.

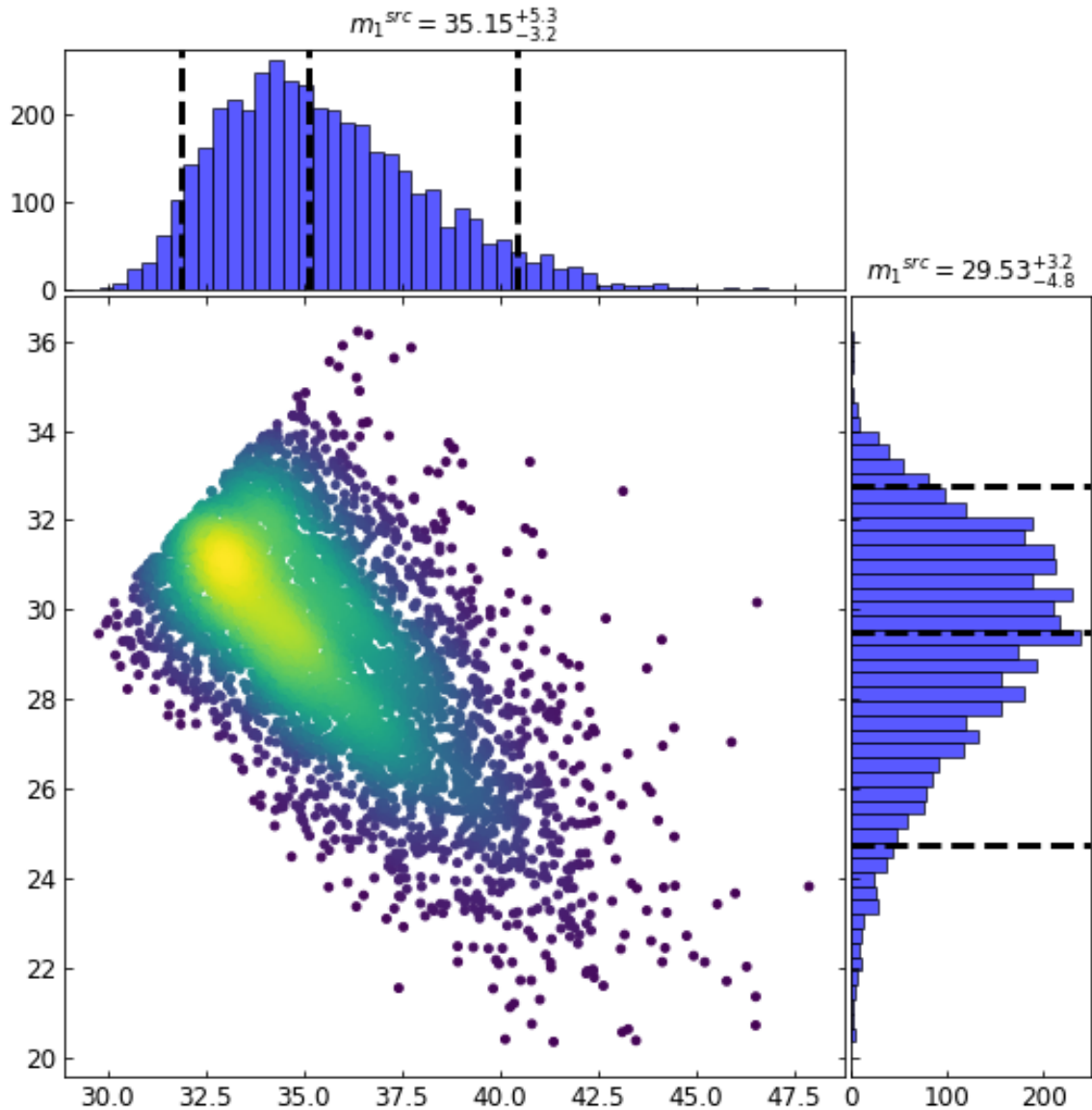


Figure 5.5: Posterior primary source mass distribution for GW150914 constructed from the posterior distributions of all three models. The sharp diagonal line in the upper left corner of the scatter plot is a consequence of the requirement that $m_1 \geq m_2$.

5.2 GW170814

GW170814 is a binary black-hole merger event that was detected on the 14th of August 2017 by both the LIGO and Virgo detectors. This event was the first gravitational-wave to be

detected by the Virgo detector. The signal to noise ratio for this event was 15.9. Table 5.2 displays the published median values with 90% confidence intervals for GW170814 [5]. This is directly followed by the results from my analysis.

Table 5.2: Median Values with 90% Confidence Intervals for Published GW170814 Parameters

| | |
|--|------------------------|
| Source-frame primary mass m_1^{source}/M_\odot | $30.5^{+5.7}_{-3.0}$ |
| Source-frame secondary mass m_2^{source/M_\odot} | $25.3^{+2.8}_{-4.2}$ |
| Source-frame chirp mass $\mathcal{M}_c^{source}/M_\odot$ | $24.1^{+1.4}_{-1.1}$ |
| Effective inspiral spin parameter χ_{eff} | $0.06^{+0.12}_{-0.12}$ |
| Source redshift z | $0.11^{+0.03}_{-0.04}$ |

5.2.1 Results

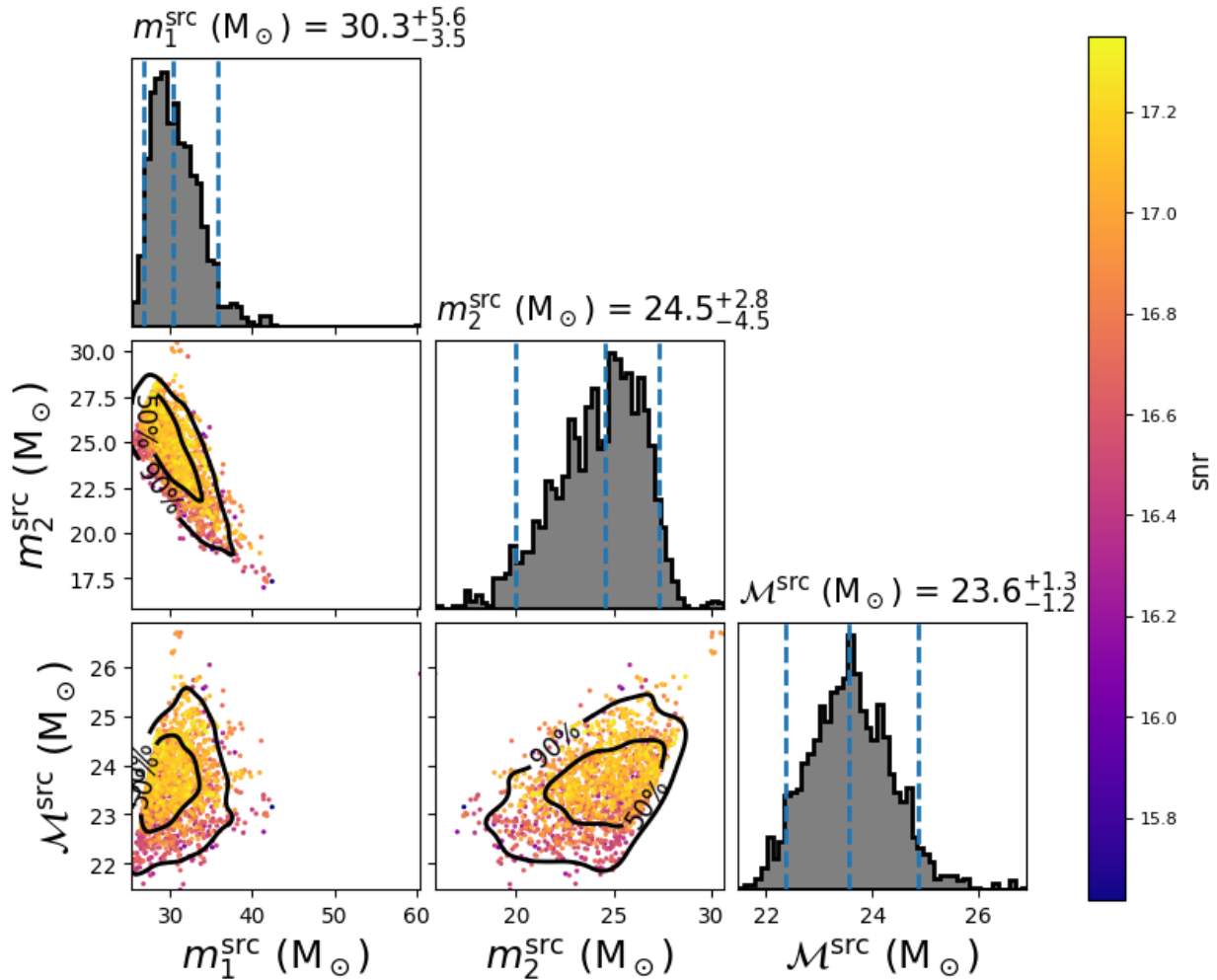


Figure 5.6: Mass Posterior Distributions for GW170814 estimated with the IMRPhenomX-PHM model.

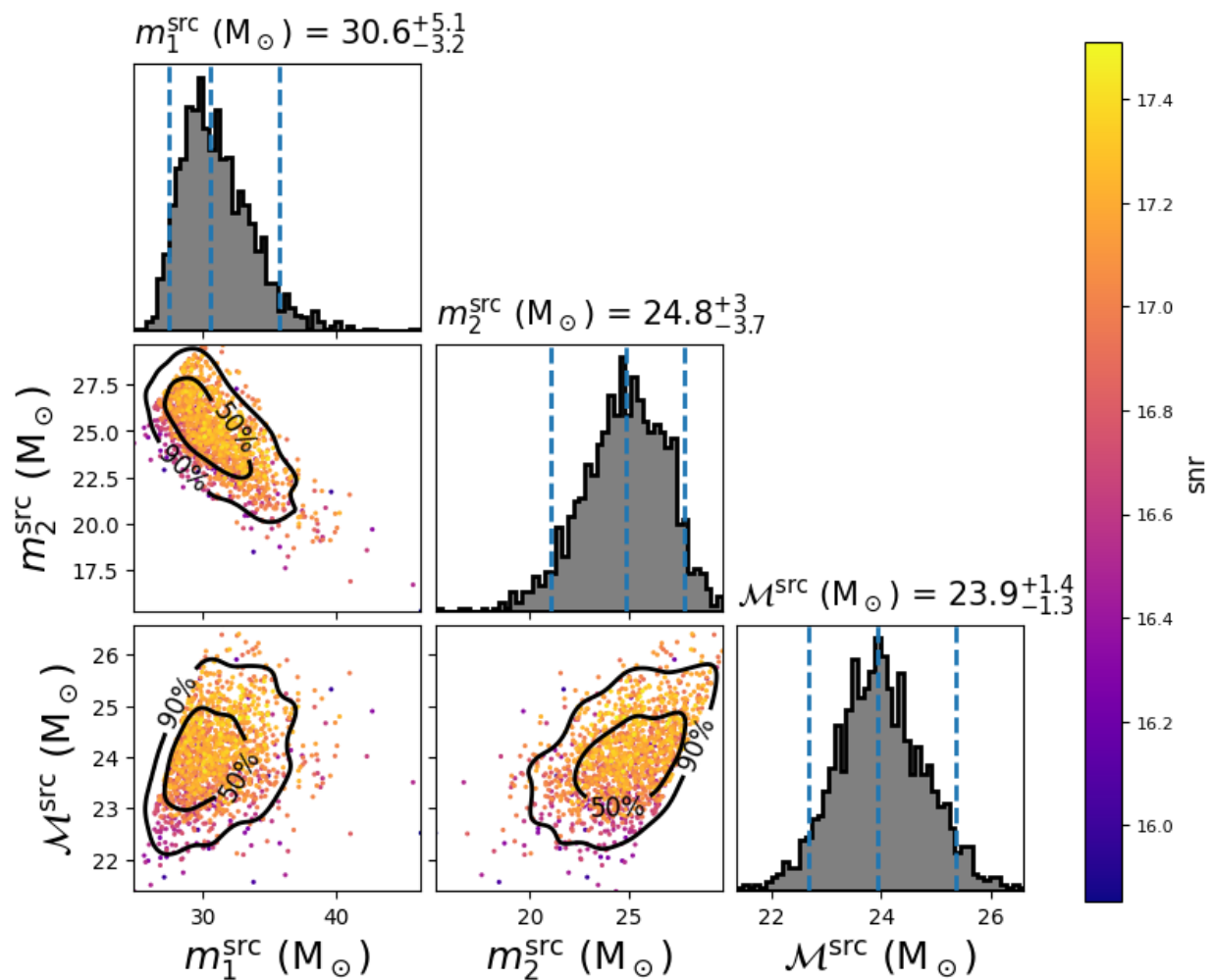


Figure 5.7: Masses for GW170814 estimated with NRSur7dq4 model.

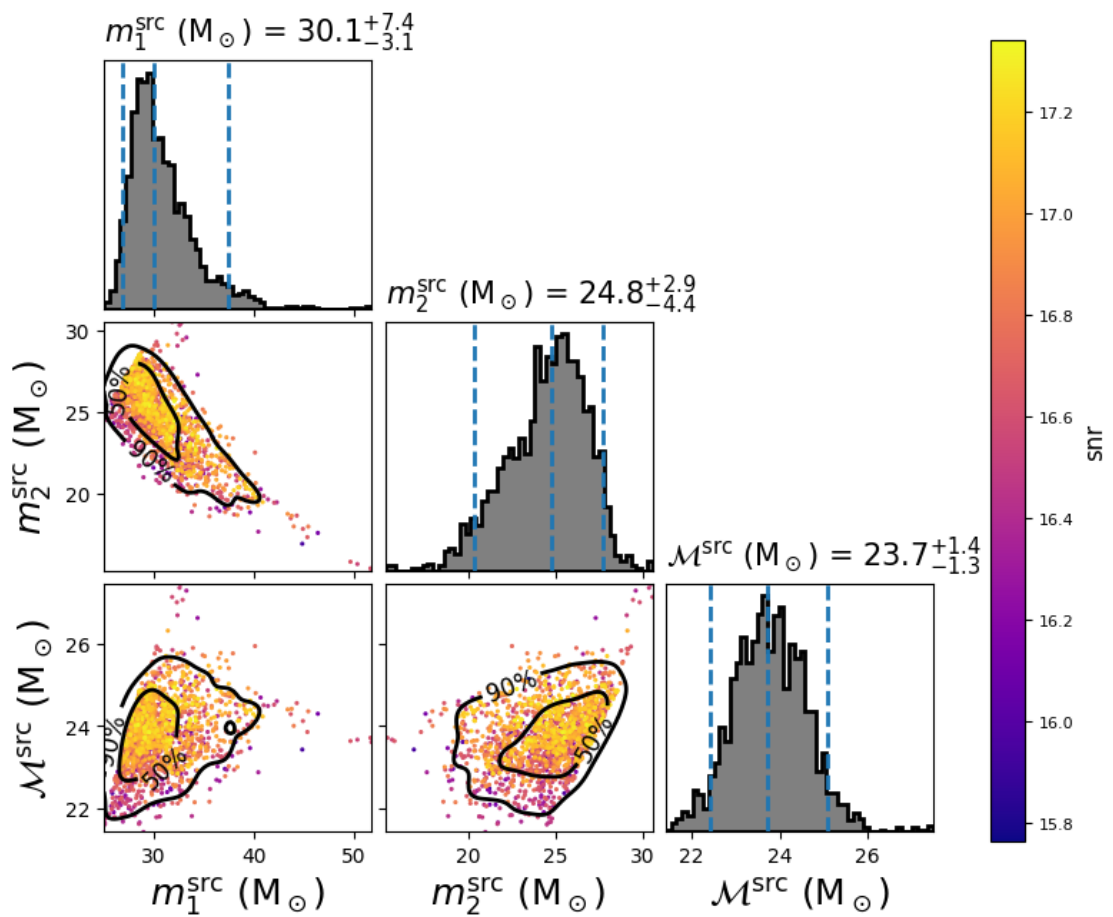


Figure 5.8: GW170814 Masses Estimated with the IMRPhenomPv2 Model

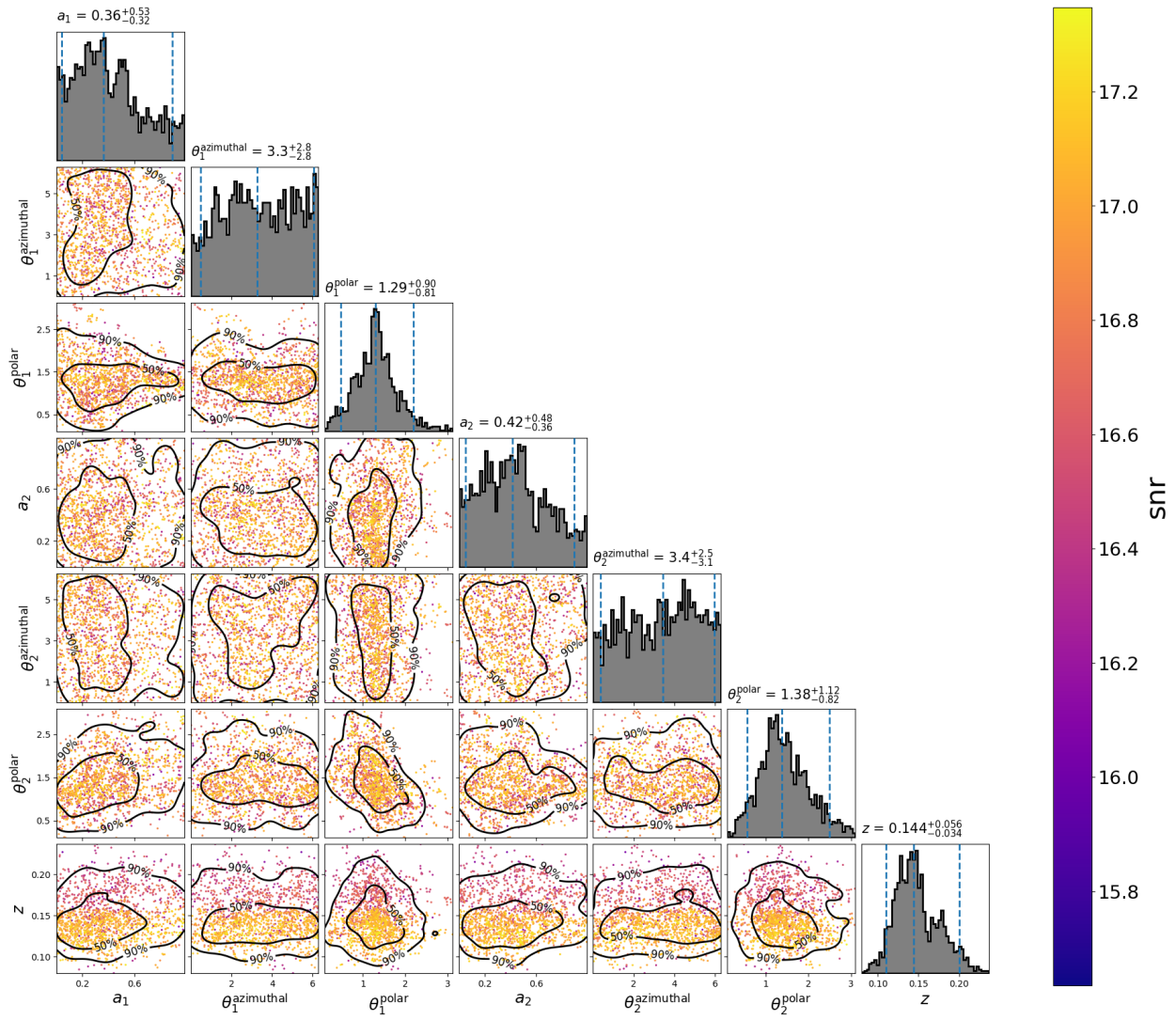


Figure 5.9: Posteriors plotted for the spins and redshift for GW170814 using the IMRPhenomXPHM Model.

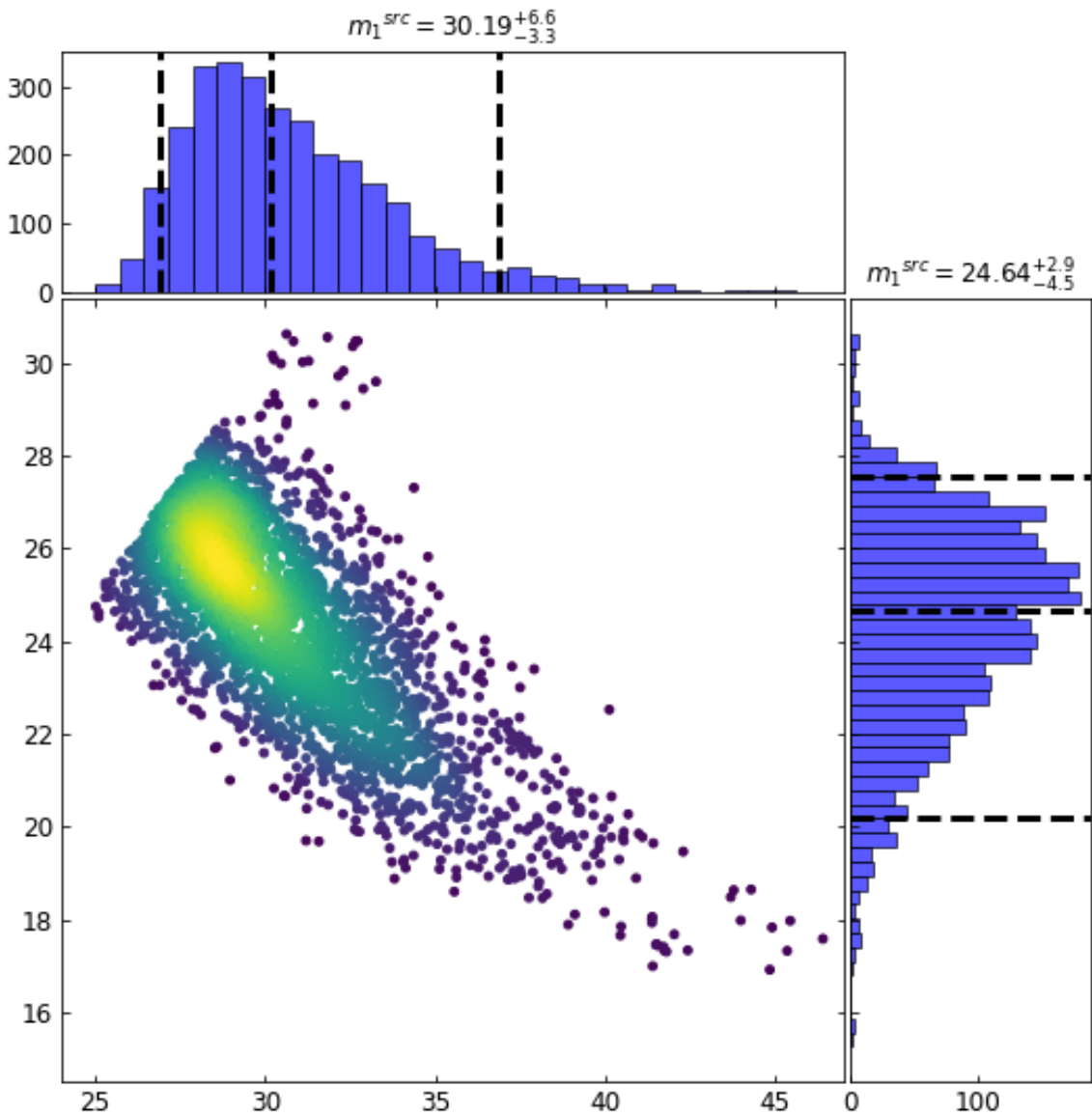


Figure 5.10: GW170814 Combined Posteriors for Masses.

5.3 GW190521B

This event was the second gravitational-wave to be detected on the 21st of May 2019. The first event garnered most of the attention as it was the heaviest and most distant black hole merger detected to date. However, the second event GW190521_074359 (henceforth GW190521B), had a much louder signal to noise ratio of 24.1 compared to 14.4. Table 5.3

displays the published median values with 90% confidence intervals for GW190521B [6]. This is directly followed by the results from my analysis of GW190521B.

Table 5.3: 90% Confidence Intervals for Published GW190521B Parameters

| | |
|--|------------------------|
| Source-frame primary mass m_1^{source}/M_\odot | $42.2_{-4.8}^{+5.9}$ |
| Source-frame secondary mass m_2^{source}/M_\odot | $32.8_{-6.4}^{+5.4}$ |
| Source-frame chirp mass $\mathcal{M}_c^{source}/M_\odot$ | $32.1_{-2.5}^{+3.2}$ |
| Effective inspiral spin parameter χ_{eff} | $0.09_{-0.13}^{+0.1}$ |
| Source redshift z | $0.24_{-0.10}^{+0.07}$ |

5.3.1 Results

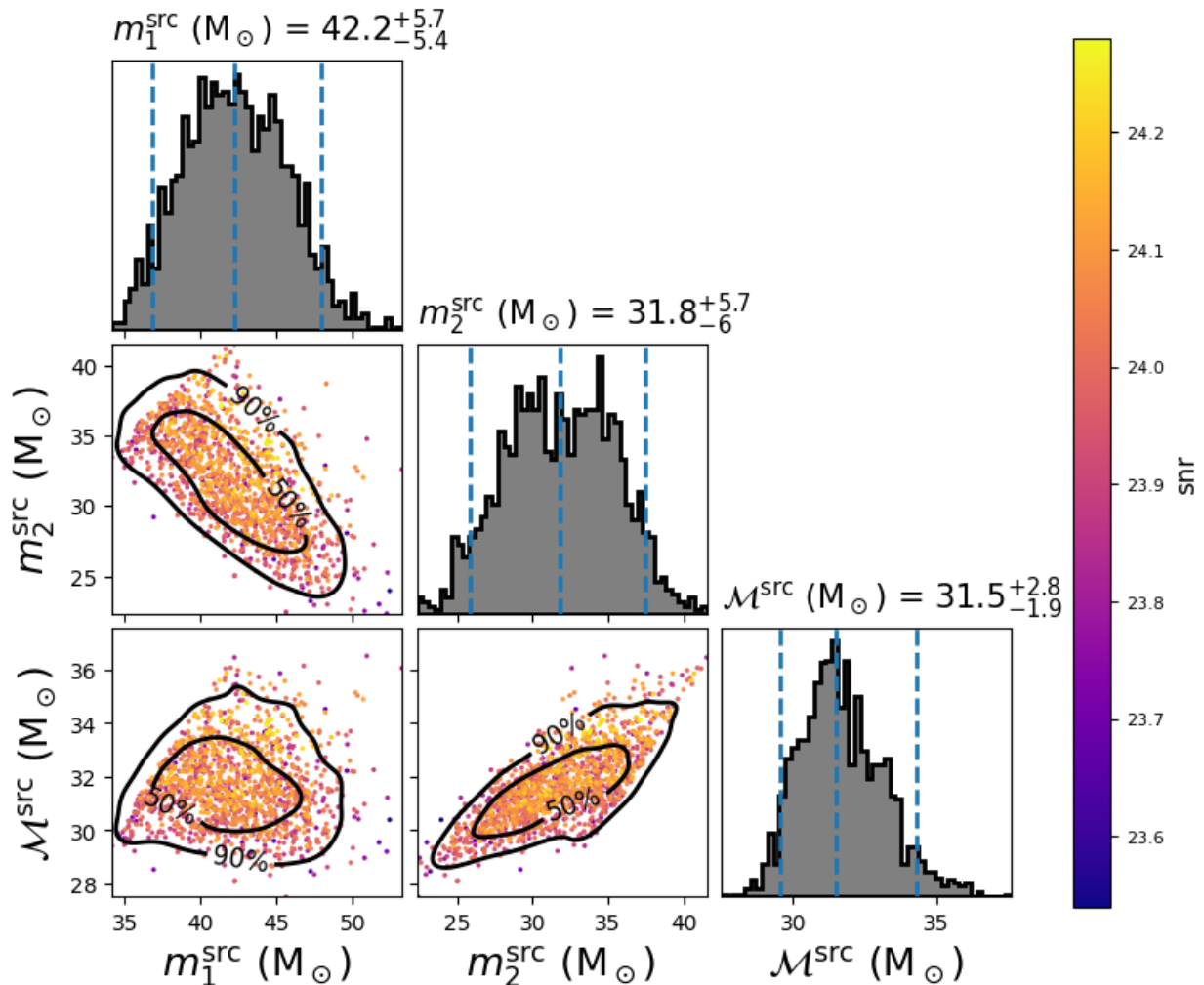


Figure 5.11: GW190521B Masses estimated with the IMRPhenomXPHM Model

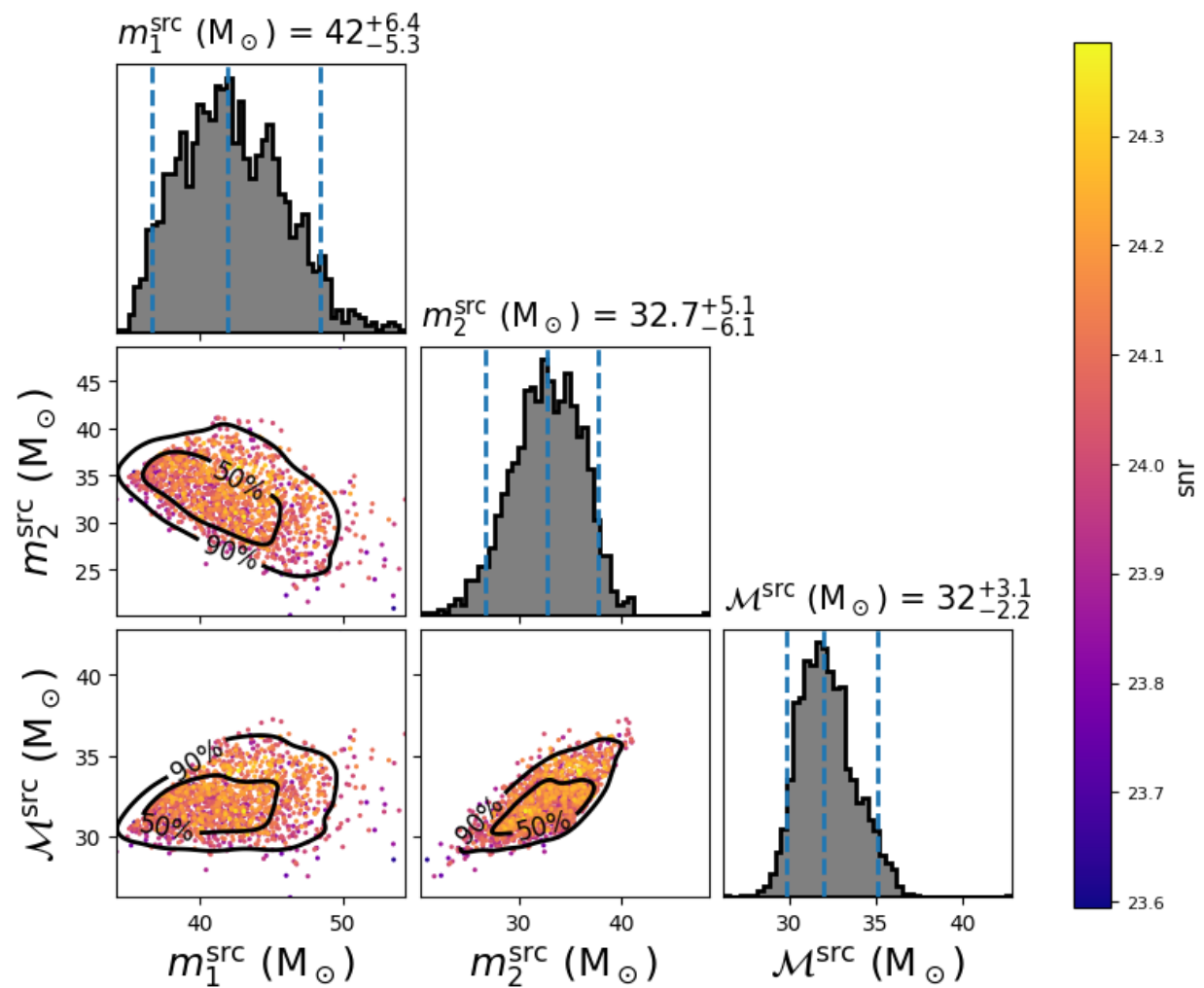


Figure 5.12: GW190521B Masses estimated with the NRSur7dq4 Model

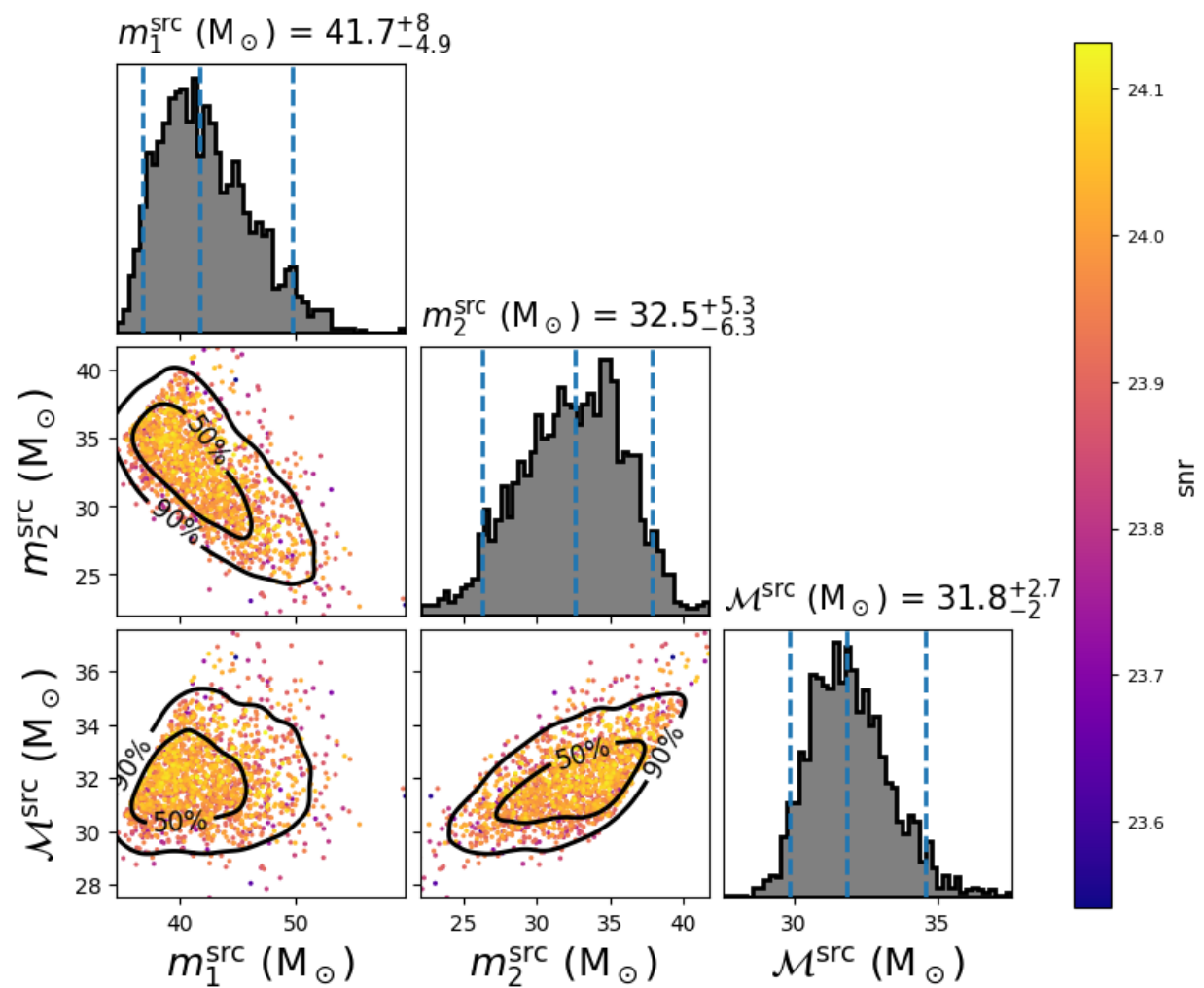


Figure 5.13: GW190521B Masses estimated with the IMRPhenomPv2 Model.

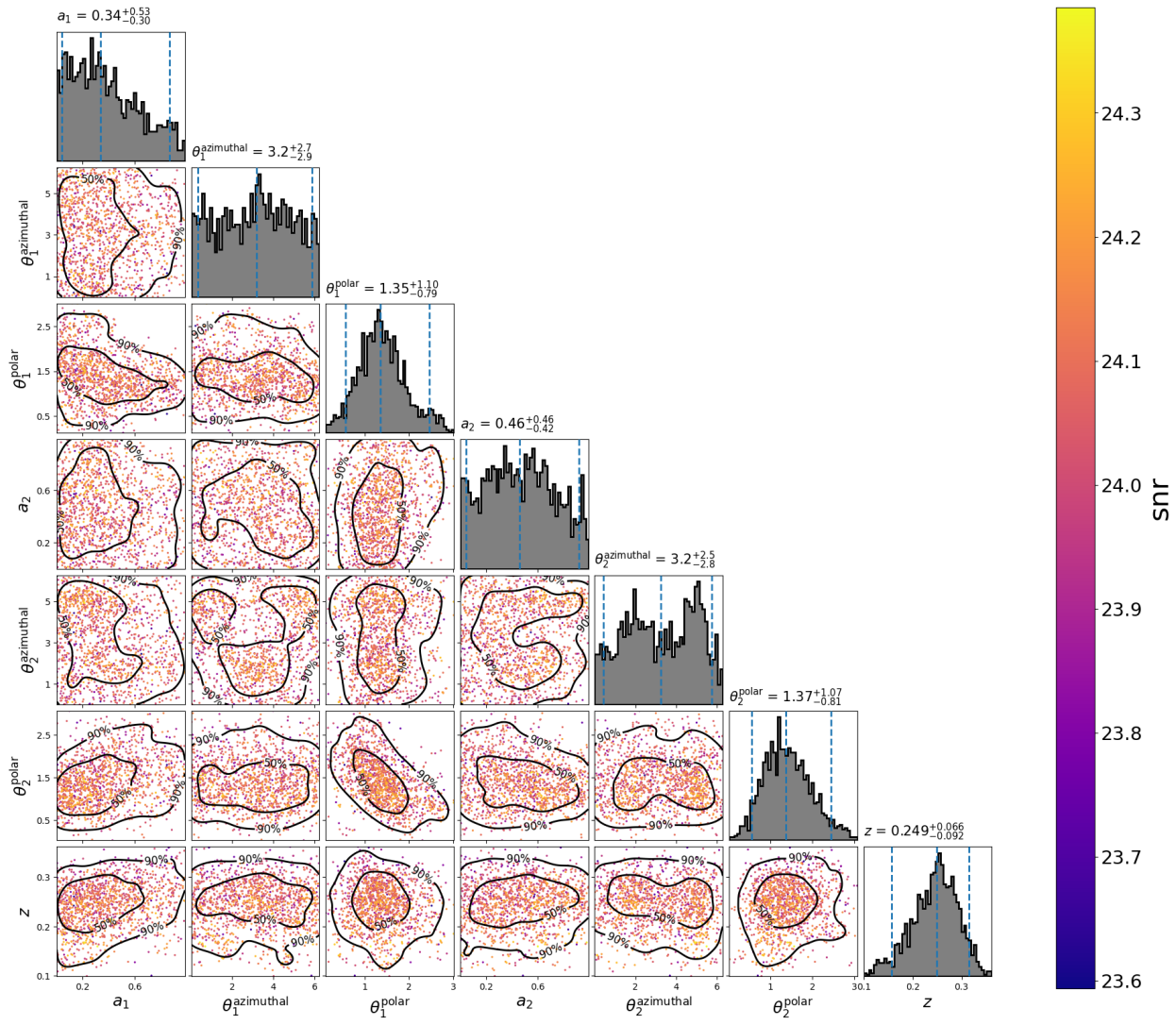


Figure 5.14: GW190521B's spins and redshift estimated with the NRSur7dq4 Model.

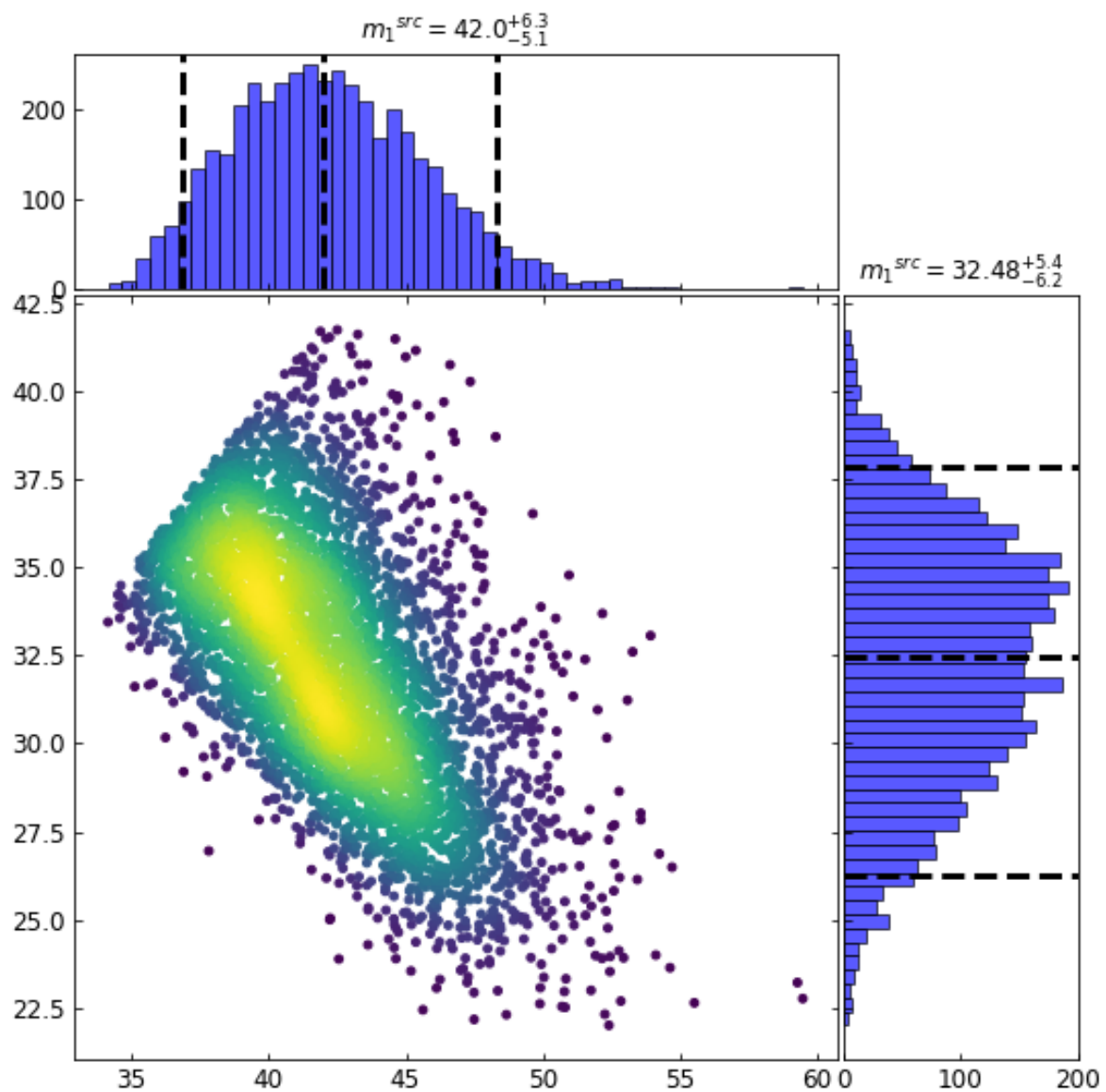


Figure 5.15: GW190521B posterior distribution for the combined source mass distributions of all three models.

Conclusions and Further Scope

The detection of gravitational-waves was another test passed with flying colours for Einstein's theory of general relativity. The field of gravitational-wave astronomy is a flourishing field that gives us a fascinating insight into the origins of our universe. However, there is still much more to learn from these detections. This project found the waveform models to produce consistent parameter estimation results for the binary black-hole merger events studied. In these estimations, we assumed the priors for the parameters to be uniformly distributed. Now with over 90 gravitational wave events detected, and their parameters estimated, we can use these posterior results to inform our prior distribution. Fig. 6.1 below is a distribution plot for the primary source mass, median values of m_1^{src} , with the data obtained from the gravitational wave open science center's website [8].

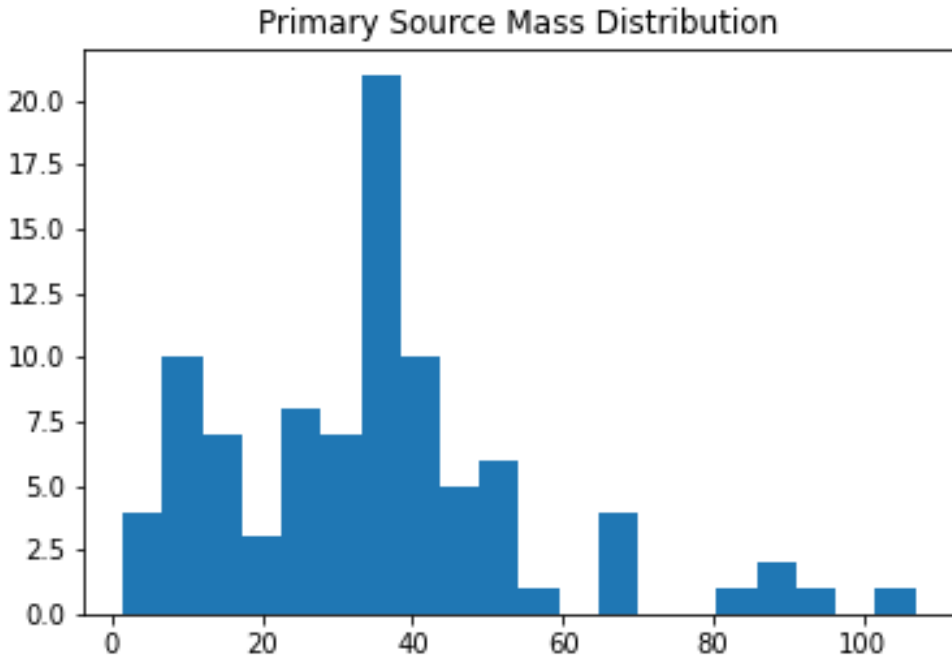


Figure 6.1: Histogram of the median value of the primary source masses for the 93 gravitational-wave events to date.

Using this data, we can estimate a probability density function for the primary source mass using a method called ‘Kernel Density Estimation’. Kernel Desnity Estimation learns the shape of the probability density function from the data. Let $X_1, \dots, X_n \in \mathbb{R}^d$ be an independent and identically distributed random sample from and unknown distribution P with density function p . We can then estimate p using,

$$\hat{p}_n(x) = \frac{1}{nh^d} \sum_{i=1}^n K\left(\frac{x - X_i}{h}\right). \quad (6.1)$$

Where,

$$K(x) = \frac{\exp(-\|x\|^2/2)}{\int \exp(-\|x\|^2/2) dx}. \quad (6.2)$$

Here h controls the amount of smoothing and K is the Gaussian kernel function [10]. Effectively kernel density estimation combines multiple Gaussian distributions of varying widths and peaks, based on the data points, together to approximate p . Fig. 6.2 below is an estimated probability density function for the primary source mass. The distribution of the masses, with the frequencies scaled, is plotted underneath for reference.

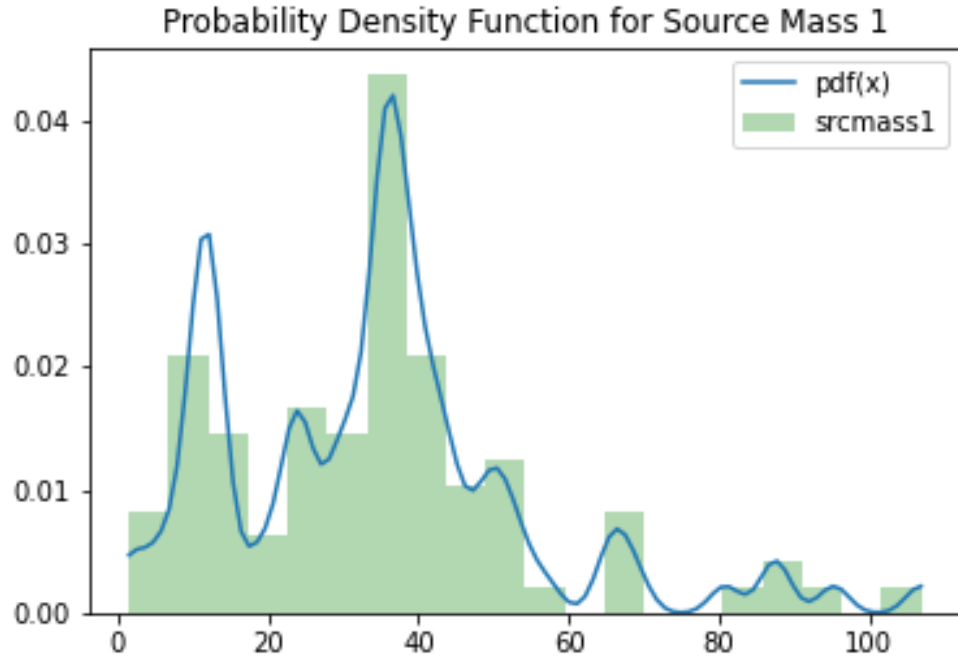


Figure 6.2: Estimated Probability Density Function for the Primary Source Mass.

This is quite a different distribution to that of the uniform distribution assumed as a prior for the events in this analysis. An interesting progression would be to extend this idea to other mass parameters and use these as priors in our estimation. This could lead to some interesting results about the posterior distributions of gravitational-wave parameters. In principle you could apply this to all the parameters estimated. However, most of the systems parameters are only loosely constrained, except for the rare events with $SNR > 20$. Therefore, it may not be an informative exercise for those parameters.

Bibliography

- [1] What are gravitational waves? <https://www.ligo.caltech.edu/page/what-are-gw>. Accessed: 2022-03-25.
- [2] What is an interferometer? <https://www.ligo.caltech.edu/page/what-is-interferometer>.
- [3] B. P. Abbott et al. Observation of Gravitational Waves from a Binary Black Hole Merger. *Phys. Rev. Lett.*, 116(6):061102, 2016.
- [4] B. P. Abbott et al. Properties of the Binary Black Hole Merger GW150914. *Phys. Rev. Lett.*, 116(24):241102, 2016.
- [5] B. P. Abbott et al. GW170814: A Three-Detector Observation of Gravitational Waves from a Binary Black Hole Coalescence. *Phys. Rev. Lett.*, 119(14):141101, 2017.
- [6] R. Abbott et al. GWTC-2: Compact Binary Coalescences Observed by LIGO and Virgo During the First Half of the Third Observing Run. *Phys. Rev. X*, 11:021053, 2021.
- [7] Sarp Akcay. Forecasting Gamma-Ray Bursts Using Gravitational Waves. *Annalen Phys.*, 531(1):1800365, 2019.
- [8] Gravitational Wave Open Science Center. Gwosc. <https://www.gw-openscience.org/eventapi/html/GWTC/>.
- [9] Jorge Cervantes-Cota, Salvador Galindo-Uribarri, and George Smoot. A brief history of gravitational waves. *Universe*, 2(3):22, sep 2016.
- [10] Yen-Chi Chen. A tutorial on kernel density estimation and recent advances. *Biostatistics Epidemiology*, 1, 04 2017.

- [11] Mark Hannam, Patricia Schmidt, Alejandro Bohé , Leila Haegel, Sascha Husa, Frank Ohme, Geraint Pratten, and Michael Pürer. Simple model of complete precessing black-hole-binary gravitational waveforms. *Physical Review Letters*, 113(15), oct 2014.
- [12] Ian Hinder, Lawrence E. Kidder, and Harald P. Pfeiffer. Eccentric binary black hole inspiral-merger-ringdown gravitational waveform model from numerical relativity and post-Newtonian theory. *Phys. Rev. D*, 98(4):044015, 2018.
- [13] Sebastian Khan, Frank Ohme, Katerina Chatzioannou, and Mark Hannam. Including higher order multipoles in gravitational-wave models for precessing binary black holes. *Phys. Rev. D*, 101(2):024056, 2020.
- [14] Tyson Bailey Littenberg. *A comprehensive Bayesian approach to gravitational wave astronomy*. PhD thesis, Montana State U., 2009.
- [15] Michele Maggiore. *Gravitational Waves. Vol. 1: Theory and Experiments*. Oxford Master Series in Physics. Oxford University Press, 2007.
- [16] Alex Nitz, Ian Harry, Duncan Brown, Christopher M. Biwer, Josh Willis, Tito Dal Canton, Collin Capano, Thomas Dent, Larne Pekowsky, Andrew R. Williamson, Soumi De, Miriam Cabero, Bernd Machenschalk, Duncan Macleod, Prayush Kumar, Steven Reyes, dfinstad, Francesco Pannarale, Sumit Kumar, Thomas Massinger, Márton Tápai, Leo Singer, Gareth S Cabourn Davies, Sebastian Khan, Stephen Fairhurst, Alex Nielsen, Shashwat Singh, Koustav Chandra, shasvath, and veronica villa. gwastro/pycbc: v2.0.2 release of pycbc, March 2022.
- [17] B. S. Sathyaprakash and B. F. Schutz. Physics, Astrophysics and Cosmology with Gravitational Waves. *Living Rev. Rel.*, 12:2, 2009.
- [18] PyCBC Development Team and the LIGO / Virgo Collaborations. Pycbc. <https://pycbc.org/>. Accessed: 2022-03-25.

- [19] Vijay Varma, Scott E. Field, Mark A. Scheel, Jonathan Blackman, Davide Gerosa, Leo C. Stein, Lawrence E. Kidder, and Harald P. Pfeiffer. Surrogate models for precessing binary black hole simulations with unequal masses. *Physical Review Research*, 1(3), oct 2019.